Supplementary Information (SI) for Nanoscale.

Supporting Information for

Design and Fabrication of Plasmonic Hedgehog-Shaped Covalent Organic Framework Nanocomposites for Indirect SERS-based Ultradetection of Water Contaminant Terbutryn

Tolga Zorlu,[a,b] Maedeh Anisi,[b] Monica Quarato,[c] Ana Vieira,[c] Jesús Giráldez-Martínez,[b] Carlos Gonçalves,[c] Aitor Alvarez,[c] Tania Prieto,[b] Dana D. Medina,[d] Lucas V. Besteiro,*[,b] Miguel A. Correa-Duarte,[b] Begoña Espiña,[c] Laura M. Salonen,*[,b,c] Laura Rodriguez-Lorenzo*[,c]

[a.] *Department of Physical and Inorganic Chemistry, Universitat Rovira i Virgili, Carrer de Marcel·lí Domingo s/n, 43007 Tarragona, Spain*

[b.] *CINBIO, University of Vigo, 36310 Vigo, Spain. E-mail: lucas.v.besteiro@uvigo.es; lauramaria.salonen@uvigo.es*

[c.] *International Iberian Nanotechnology (INL), Avenida Mestre José Veiga, 4715-330 Braga, Portugal. E-mail: laura.rodriguez-lorenzo@inl.int*

[d.] *Department of Chemistry and Center for Nanoscience (CeNS), Ludwig-Maximilians-University, Butenandtstraße 11 (E), 81377 Munich, Germany*

EXPERIMENTAL SECTION

1. Materials and methods

Chemicals

2,5-Dimethoxyterephthalaldehyde (97%, DMTP), 1,3,5-tris(4-aminophenyl)benzene (97%, TAPB), gold(III) chloride trihydrate (99.9%, $HAuCl_4 \cdot 3H_2O$), sodium citrate tribasic dihydrate (≥98%, CA), poly(allylamine hydrochloride) (M_w = 15000 Da, PAH), 4-aminothiophenol (≥97%, 4-ATP), 4-nitrothiophenol (4-NTP), terbutryn, ammonium hydroxide (28–30%, NH_4OH), acetonitrile, acetic acid (AcOH), acetone (99.5%), tetrahydrofuran (99.9%, THF) and ethanol (99.5%) were purchased from Sigma–Aldrich. Tetraethyl orthosilicate (98%, TEOS) was purchased from Acros Organics. All reactants were used without further purification. Milli-Q water (18 MΩ cm^{-1}) was used in all aqueous solutions, and all the glassware was cleaned with aqua regia before the experiments

Instrumentation

UV–vis spectroscopy (Agilent Technologies, Cary 8454), transmission electron microscopy (TEM) (JEOL JEM 1010), scanning electron microscopy (SEM) (Helios NanoLab 600) operating at an acceleration voltage of 100 kV were applied to characterize the optical response and size of the particles. The samples were prepared by drying suspensions on carbon–Formvar–coated 200–mesh copper grids. Zeta potential studies were carried out with a Malvern Zetasizer Nano ZS instrument. The zeta potential was calculated from electrophoretic mobility using the Smoluchowski approximation. Nitrogen physisorption was carried out with N_2 at 77 K using a Flex & 3Flex Adsorption Analyzer from Micromeritics. Before analysis, the samples were outgassed at room temperature for 12 h under a pressure of 0.1 Pa. The Brunauer–Emmett–Teller (BET) analysis was carried out in the relative pressure range of 0.05–0.25. Powder X-ray diffraction

(PXRD) analysis was carried out with a Siemens D5000 instrument. The patterns were obtained on a Bruker D8 Advance diffractometer in Bragg–Brentano geometry equipped with a Cu Kα source (0.1 mm divergence slit, knife edge air scatter screen) and a LynxEye detector. Kβ radiation was attenuated with a 0.0125 mm Ni filter. Raman and SERS spectra were collected in backscattering geometry with a Renishaw inVia Reflex system equipped with a 2D-CCD detector, a Leica confocal microscope, and two excitation sources: a 532 nm frequency doubled Nd:YAG/Nd:YVO_4 diode, and a 785 nm NIR diode laser.

Computational methods

Volume and cross sectional area of the probe molecules were calculated with density functional theory (DFT) at the B3LYP 6-311G(d,p) level of theory using Gaussian 16 [1].

2. Synthetic Procedure

Preparation of $COF_{Hedgehog}$ Particles

DMTP (19.4 mg, 0.1 mmol) and TAPB (23.5 mg, 0.067 mmol) were added to 20 mL of acetonitrile at room temperature and under air. The mixture was stirred for 5 min at 250 rpm, and then, 0.8 mL of aq. AcOH solution (12 M) were added. The colour of the solution changed first to greenish and then yellow. The solution was kept stirring for 72 h. For washing, 20 mL of THF was added, and the mixture was sonicated for 5 min. Then, the particles were sedimented by centrifugation under 13000 rpm for 5 min. Finally, the particles were washed with acetone 5–6 times and collected by centrifugation as described above, redispersed in acetone, and dried under N_2 atmosphere.

Preparation of COF_{Bulk}

For the preparation of COF_{Bulk}, DMTP (19.4 mg, 0.1 mmol) and TAPB (23.5 mg, 0.067 mmol) were dispersed in 20 mL of acetonitrile, and then, 0.8 mL of aq. AcOH (12 M) were further added. The reaction vessel was put to the oven for 72 h at 120 °C. Then, the reaction was cooled down to the

room temperature, COF_{Bulk} was sedimented with centrifugation under 13000 rpm for 5 min. Finally, COF_{Bulk} was washed with acetone 5–6 times and collected by centrifugation as described above, redispersed in acetone, and dried under N_2 atmosphere.

Preparation of Au Seeds

Au seeds were synthesized according to the well-known Turkevich method [2, 3]. Briefly, 5 mL of an aqueous 34 mM CA aqueous were added to 100 mL of a boiling aqueous 0.5 mM $HAuCl_4$ solution under vigorous stirring. The boiling mixture was allowed to react for 1 h under stirring. The synthesis yielded spherical Au NPs of about 13–15 nm in size. [Au]: 1.16 mM and [NP]: 17.1 nM.

Deposition of Au NPs on SiO_2 (SiO_2@Au) Beads

SiO_2 beads were prepared according to the Stöber method [4, 5]. Briefly, 1.96 mL NH_4OH (28–30%) were added to an ethanol–H_2O mixture (3.21 mL H_2O and 18.12 mL EtOH). Then, 1.71 mL TEOS were added, and the mixture was stirred at 700 rpm for 2h. For purification, the particles were sedimented with a centrifuge under 2500 rpm for 15 min, and washed with ethanol four times (4000 rpm, 10 min), and finally, redispersed in ethanol.

Before the preparation of SiO_2@Au, the beads of ca. 500 nm diameter were coated with positively charged PAH. To this end, 10 mg of PAH were added to 5 mL of water and sonicated for 30 min. Then, 2 mL of the SiO_2 bead dispersion (1 mg/mL) were added to PAH aqueous solution and stirred at 500 rpm for 2 h. The sample was then submitted to three centrifugation–washing cycles (9000 rpm, 30 min) with Milli–Q water to remove unbound PAH. Finally, the SiO_2/PAH beads were redispersed in 2 mL of Milli–Q water ([SiO_2] = 1 mg/mL).

To prepare SiO_2@Au beads, SiO_2 bead solution was added dropwise to 100 mL of the Au colloids ([Au] = 1.16 mM) under sonication for 30 min. Immediately after, the mixture was stirred (300 rpm) overnight. Finally, the mixture was submitted to three centrifugation–washing cycles (4500 rpm,

30 min) with Milli–Q water to remove unbound Au NPs. The resulting SiO_2@Au beads were redispersed in 20 mL of Milli–Q water ([SiO_2@Au] = 0.1 mg/mL).

Preparation of SiO_2@Au@$COF_{Hedgehog}$ Composite

A solution of 4-ATP (0.1 mM) in EtOH (10 mL) was added to an aqueous SiO_2@Au bead (0.1 mg/mL; 10 mL) solution. The mixture was stirred overnight to maximize the adsorption of 4-ATP to the NP surface. Then, the particles were washed once (4500 rpm, 30 min) with acetonitrile and redispersed in 10 mL of acetonitrile. A solution of DMTP (19.4 mg, 0.1 mmol) in 10 mL of acetonitrile was added to the SiO_2@Au bead solution. The mixture was stirred for 5 min at 250 rpm, and then 0.8 mL of aqueous 12 M AcOH solution were further added, and the mixture was stirred at room temperature overnight. Thereafter, the resulting DMTP-functionalized-SiO_2@Au beads were sedimented (4500 rpm, 30 min) and redispersed in 10 mL of acetonitrile. After this step, 3.8 mg of DMTP (0.02 mmol) and 4.7 mg of TAPB (0.0134 mmol) were dissolved in 2 mL of acetonitrile, added to the bead solution and the mixture was sonicated for 10 min. Then, 0.16 mL of aqueous 12 M AcOH solution was added, and the mixture was sonicated for additional 5 min. Finally, the mixture was stirred for 72h at 250 rpm. For washing, 12 mL of THF were added, and the mixture was sonicated for 5 min. Then, the particles were sedimented with centrifugation under 9000 rpm for 5 min. Finally, the particles were washed with acetone 5–6 times, collected by centrifugation as described above, and redispersed in water ([SiO_2@Au@$COF_{Hedgehog}$] = 0.1 mg/mL).

In situ Preparation of COF@Au Composites

For the *in situ* preparation, 1 mg of $COF_{Hedgehog}$ particles were added to 25 mL of $HAuCl_4$ solution (0.5 mM) and left overnight to maximize the absorption of gold salt. Then, the transparent supernatant was discarded, and the particles were dispersed in 1 mL of water ($[COF]_{final}$: 1 mg/mL). The dispersion was heated to 50-60^{0}C and to this solution, 1.25 mL sodium citrate

(10 mg/mL) was added. The mixture was stirred for 5 min at a lower speed and then left to sediment for overnight. Then, it was washed with water 3 times.

Sample Preparation for SERS Analysis

1 µL of SiO_2@Au@$COF_{Hedgehog}$ composites (0.1 mg/mL) was added to 10 mL of ethanolic solutions of 4-NTP at the desired concentration. The mixtures were incubated for 1 h and then subjected to one centrifugation–washing cycle (6000 rpm, 10 min) with Milli-Q water and redispersed in 1 mL of Milli–Q water. An identical protocol was applied for SiO_2@Au plasmonic beads. For terbutryn detection, 1 µL of 4-NTP-functionalised SiO_2@Au@$COF_{Hedgehog}$ composites was combined with 10 mL of terbutryn solution at different concentrations. The mixtures were incubated for 1 h and then subjected to a centrifugation–washing cycle (6000 rpm, 10 min) with Milli-Q water and were finally redispersed in 1 mL of Milli–Q water.

Terbutryn Adsorption

Adsorption experiments were performed by spiking an aqueous dispersion of each COF (COF_{Bulk} and $COF_{Hedgehog}$) (1 mg/mL) in ultrapure water with 150 ug/L of terbutryn. These mixtures were incubated at 19 C for 45 min under shaking. After adsorption, COFs were separated by centrifugation and subsequently, a desorption of terbutryn using ethanol was performed. The desorbed solution was analyzed by HPLC-DAD for quantification. This quantification was performed using an LC-MS/MS instrument equipped with an XSelect Premier HSS T3 (2.1 mm i.d. x 100 mm, 2.5 µm particle size) analytical column attached to the respective pre-column (2.1 mm i.d. x 5 mm, 2.5 2.5 µm particle size) (Waters, Milford, Massachusetts, USA). The mobile phases were Milli-Q water and LC-MS grade acetonitrile. The detection of terbutryn using a UV detector (DAD - Diode Array Detector) was performed at 220 nm.

Reproducibility Assessment Across Three Independent Synthetic Batches

Three independent batches of $COF_{Hedgehog}$ particles were synthesized following the procedure described in Preparation of $COF_{Hedgehog}$ Particles, and their reproducibility was assessed via PXRD and FESEM analyses.

PXRD Analysis and FWHM Variability

To evaluate the reproducibility of the $COF_{Hedgehog}$ crystallization process, PXRD patterns were collected for three independent synthetic batches (Batch 1–3). For each batch, the full width at half maximum (FWHM) of the reflection at $2\theta \approx 2.79°$ was determined using Pseudo-Voigt fitting. The obtained FWHM values showed minimal batch-to-batch variation, with a relative standard deviation (RSD%) of 7.7% (inter-batch), confirming consistent crystallinity across independent syntheses. All PXRD patterns and FWHM values for each batch are summarized in Figure S1C and Table S1 respectively.

Table S1: FWHM values for three independent $COF_{Hedgehog}$ batches

Parameter	***Batch 1***	***Batch 2***	***Batch 3***	***RSD (%)***
FWHM (2θ°)	0.336	0.301	0.29	7.7

FESEM-Based Particle Size Analysis

Particle size distributions were determined from FESEM micrographs for each batch. Sixty particles per batch were randomly selected to provide statistically meaningful measurements. The mean particle size ± standard deviation (SD) for Batch 1–3 was 241 ± 13.1 nm, 347.3 ± 19.1 nm, and 326.6 ± 23.5 nm, respectively. The intra-batch RSD% ranged from 5.45% to 7.19%, indicating consistent particle size within each synthetic batch. The FESEM images and summary statistical values are shown in figure S1e-f and Table S2.

Table S2**:** Summary of FESEM-based particle size measurements.

Sample	***Particle Size (nm)***	***SD (nm)***	***RSD (%)***
Batch 1	241 nm	13.1	5.45
Batch 2	347.3 nm	19.1	5.51
Batch 3	326.6 nm	23.5	7.19

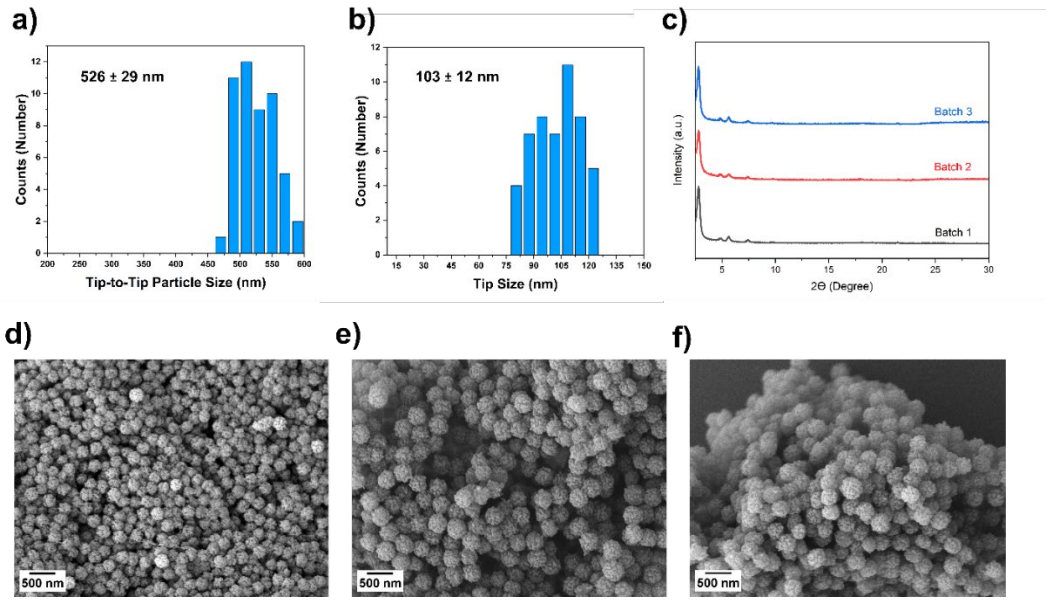

Figure S1. a) Tip-to-tip particles size, and **b)** tip size histograms of $COF_{Hedgehog}$ particles **c)** PXRD patterns of three independent $COF_{Hedgehog}$ batches. FESEM images of $COF_{Hedgehog}$ particles for **d)** Batch 1, **e)** Batch 2, and **f)** Batch 3.

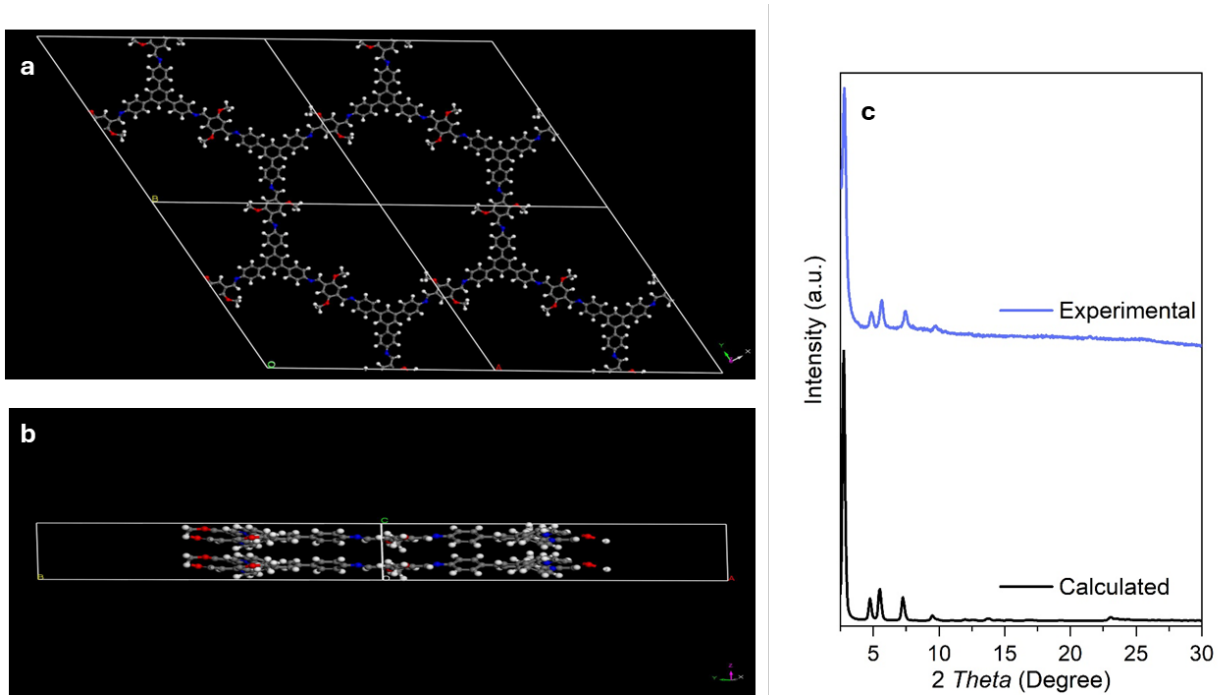

Figure S2. Simulation of the crystal unit cell calculated in an eclipsed arrangement AA: **a)** top view on AB plane; **b)** view of the COF layer stacking (located along the crystal c-axis) where the TAPB peripheral benzene rings are rotating out of plane due to steric considerations giving rise to an interlayer distance of about 3.8 Å; **c)** experimentally obtained and the simulated PXRD patterns for TAPB-DMTP.

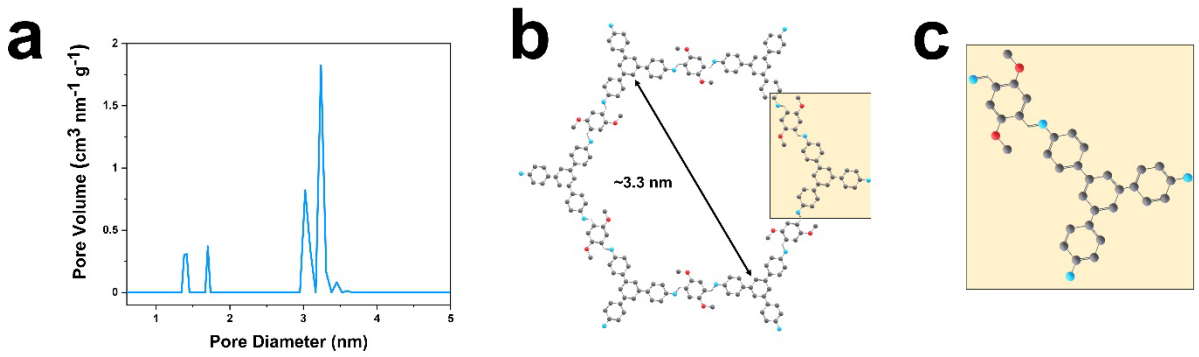

Figure S3. a) BJH pore size analysis of $COF_{Hedgehog}$ particles. **b)** Structural arrangement and pore size of DMTP-TAPB COF, and **c)** a zoom-in to the covalent bonding of monomers. Color code: grey = carbon, cyan = nitrogen, and red = oxygen.

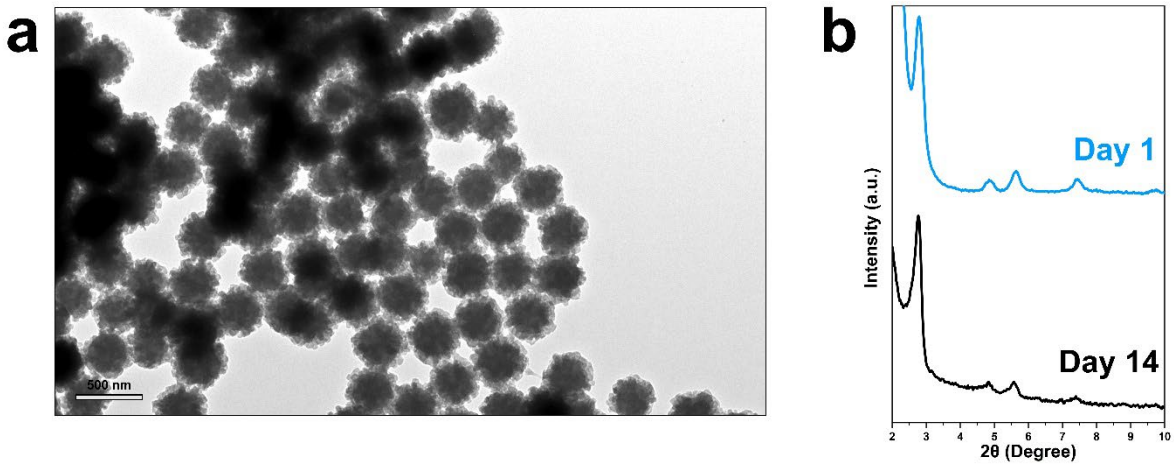

Figure S4. a) TEM images of $COF_{Hedgehog}$ particles in water after 14 days, and **b)** comparison of powder XRD patterns of the particles at day 1 and day 14.

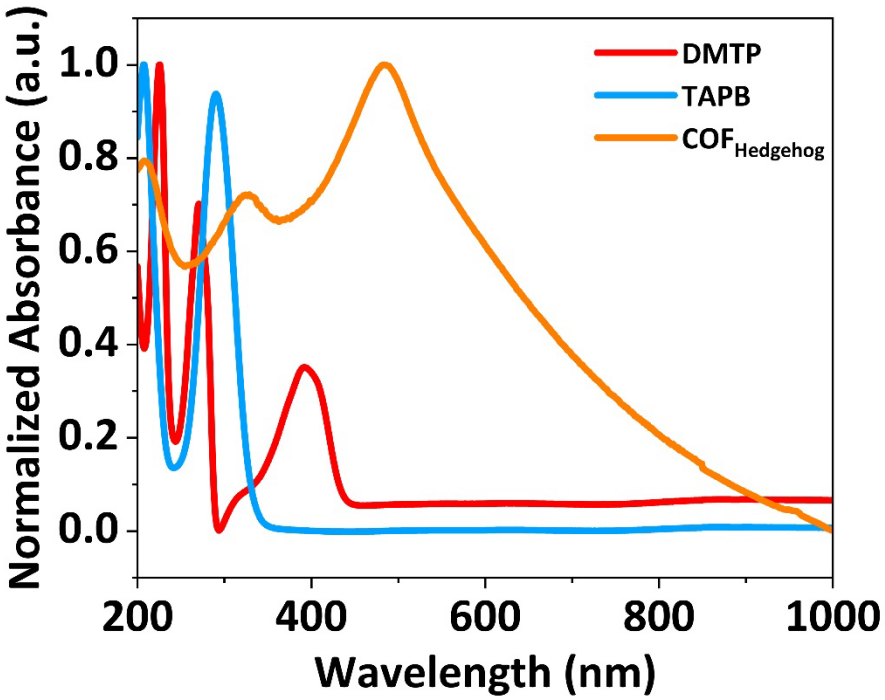

Figure S5. UV-vis spectra of the monomers and $COF_{Hedgehog}$ particles in acetonitrile.

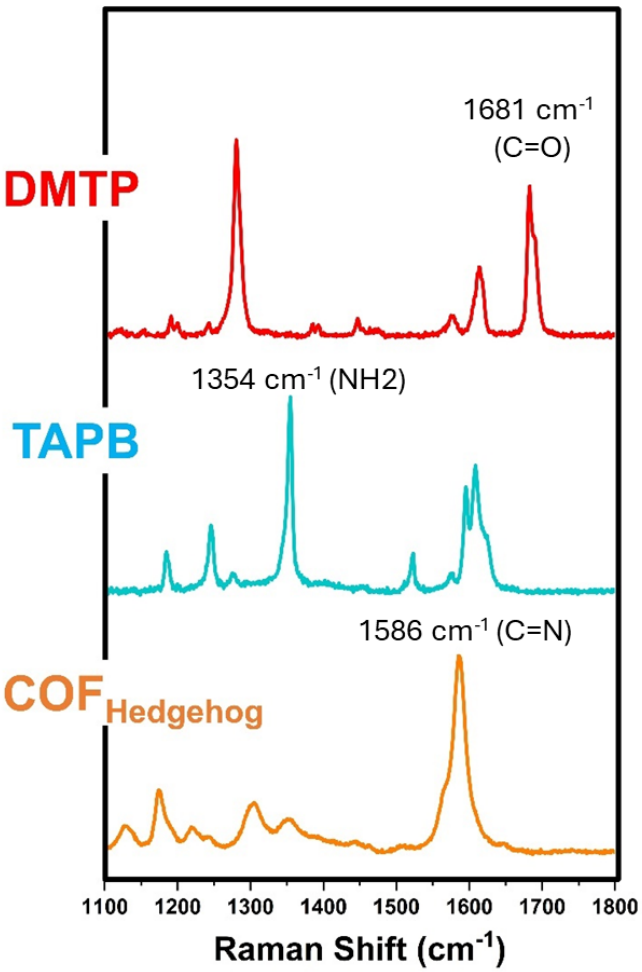

Figure S6. Raman spectra of DMTP, TAPB, and $COF_{Hedgehog}$ particles.

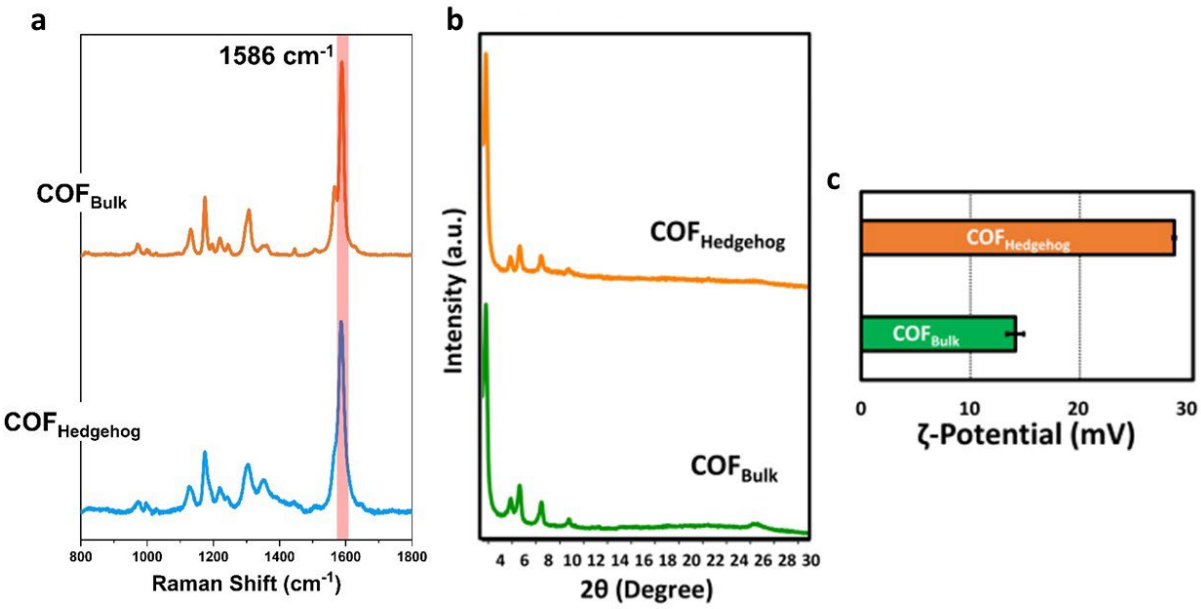

Figure S7. Comparison of **a)** Raman spectra, **b)** PXRD patterns, and **c)** Zeta potential graph of COF_{Bulk} and $COF_{Hedgehog}$ particles.

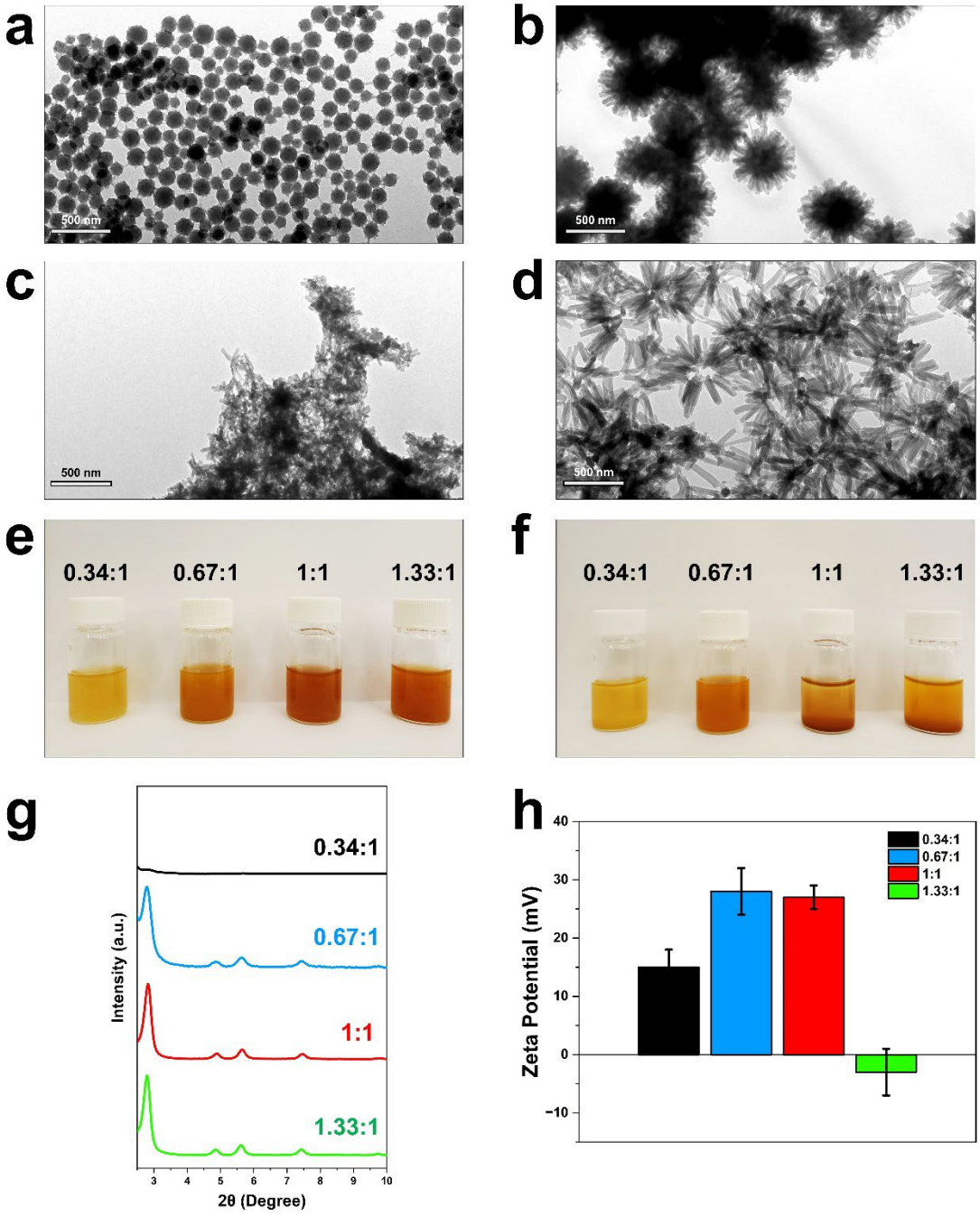

Figure S8. TEM images of COF particles prepared with different monomer [TAPB]/[DMTP] ratios: **a)** 0.34:1, **b)** 0.67:1, **c)** 1:1, and **d)** 1.33:1. **e–f)** Stabilities of COF particle dispersions in water at 0 and 1 h, respectively. **g)** PXRD patterns of COF particles. **h)** Zeta potential of COF particles with ± standard deviations.

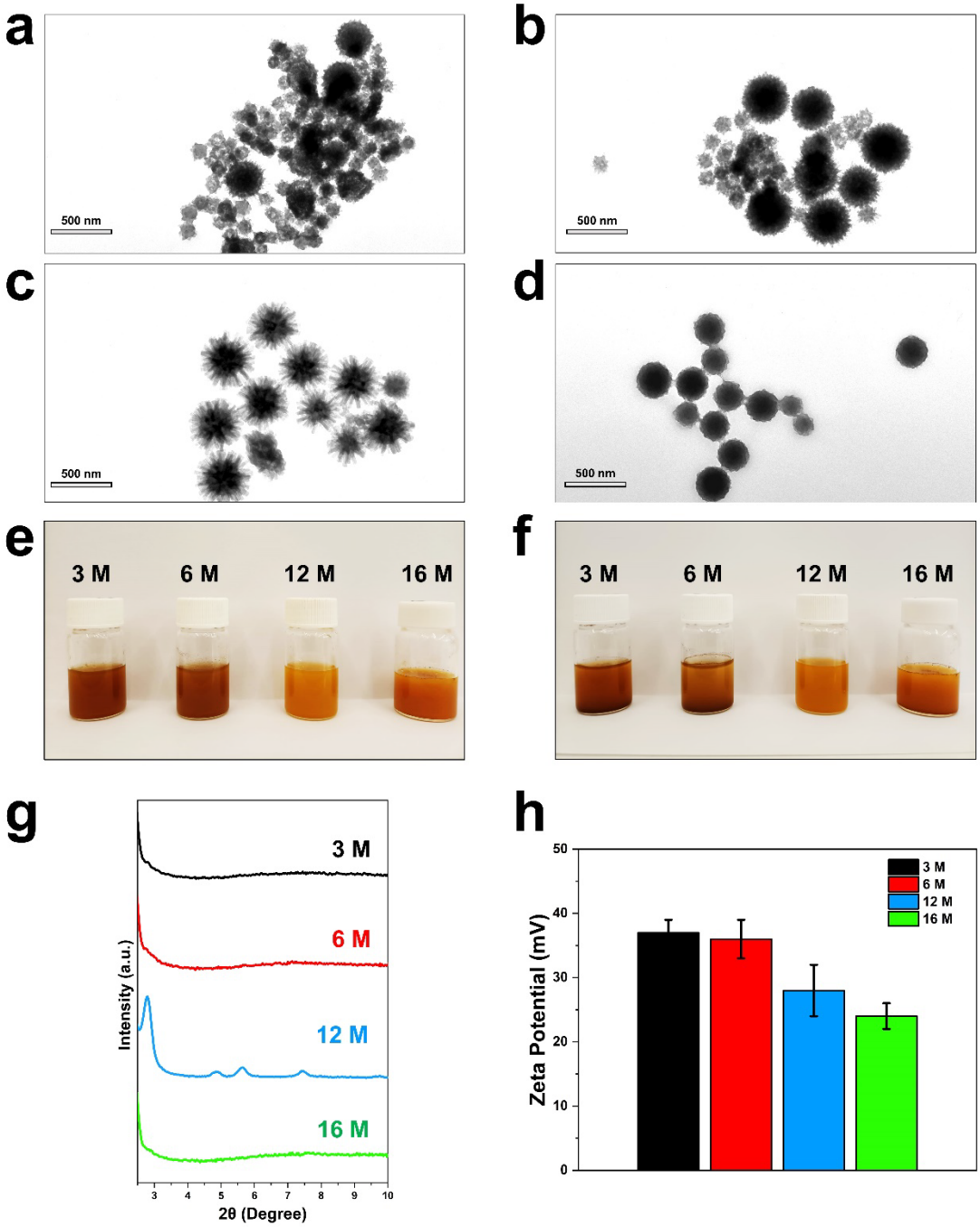

Figure S9. TEM images COF particles prepared with different AcOH concentrations: **a)** 3 M, **b)** 6 M, **c)** 12 M, and **d)** 16 M. **e–f)** Stabilities of COF particle dispersions in water at 0 and 1 h, respectively. **g)** PXRD patterns of COF particles. **h)** Zeta potential graph of COF particles with ± standard deviations.

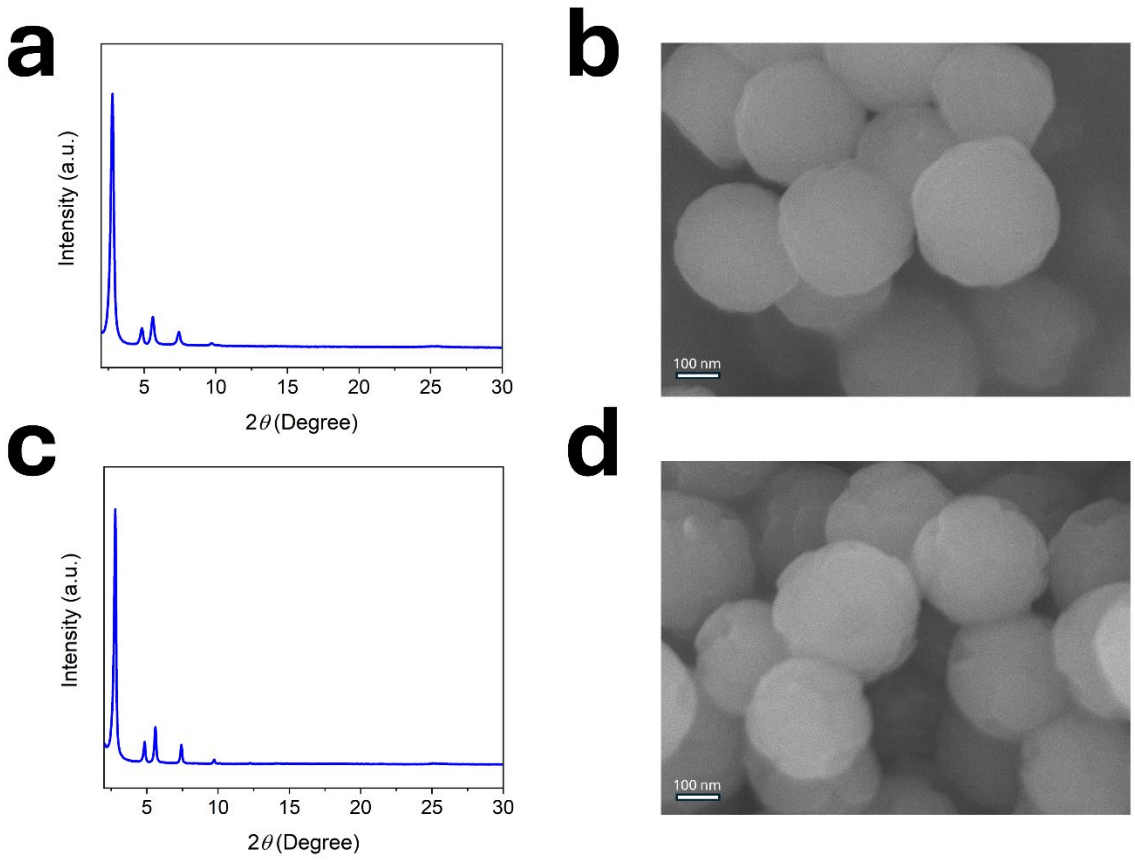

Figure S10. PXRD patterns and FE-SEM images of the effect of solvent and temperature on COF particle. **a, b)** COF synthesized using a 2:1 acetonitrile/benzonitrile mixture at room temperature. **c, d)** COF synthesized at 80 °C with acetonitrile.

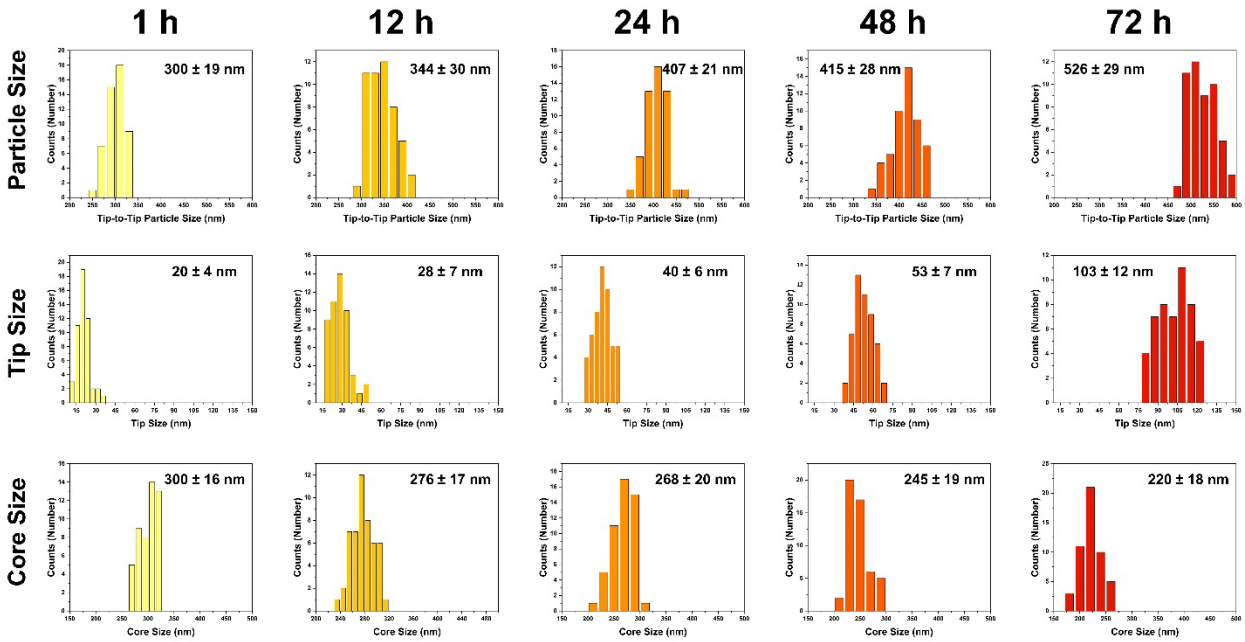

Figure S11. Morphological evolution of $COF_{Hedgehog}$ particles over time.

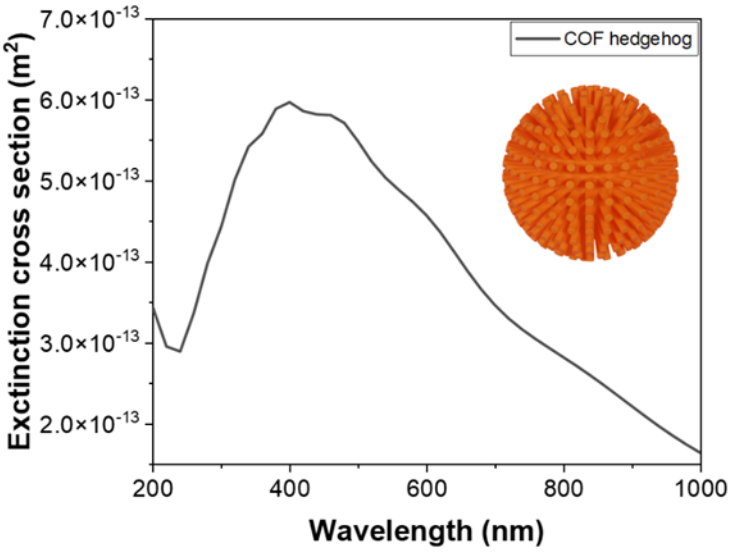

Figure S12. Simulated extinction (scattering) spectrum of the $COF_{Hedgehog}$ immersed in water, and a 3D render of the geometry used for the calculations. The size of the different parts of the geometry are described in the Theoretical methodology section, below.

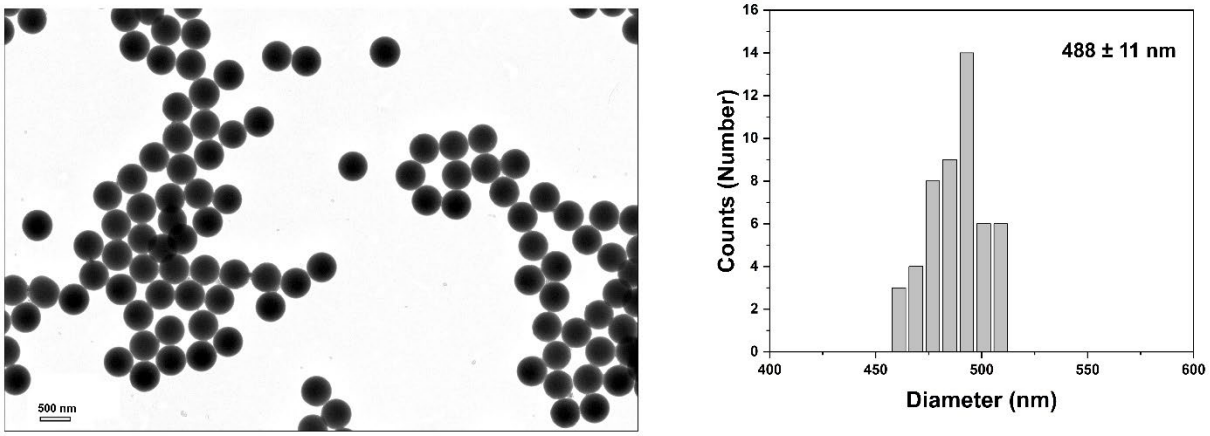

Figure S13. TEM images and size histogram of SiO_2 beads.

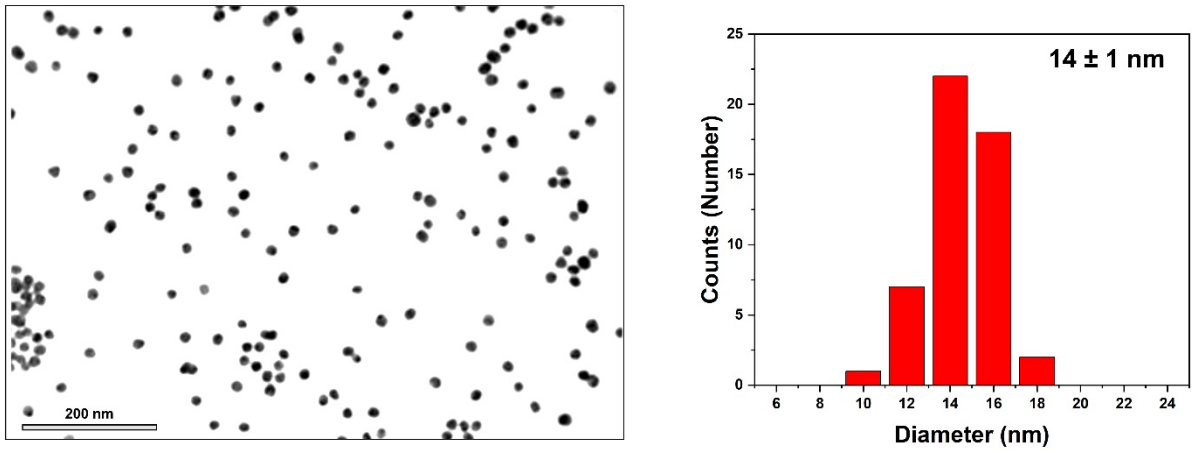

Figure S14. TEM images and size histogram of Au NPs.

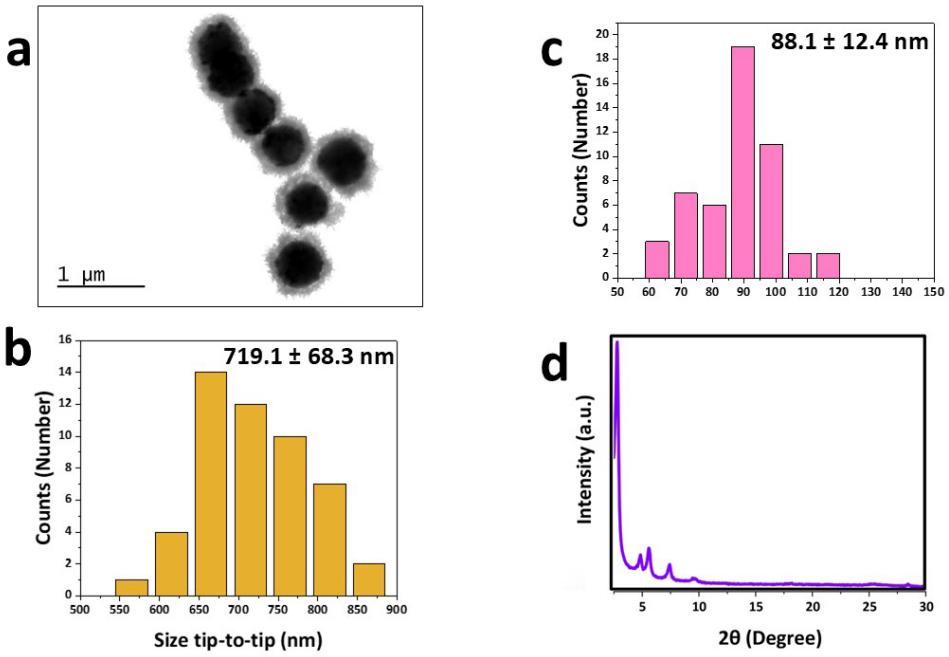

Figure S15. a) TEM images of SiO_2@Au@$COF_{Hedgehog}$ composites. **b)** Tip-to-tip particle size histogram of SiO_2@Au@$COF_{Hedgehog}$ composites. **c)** Thickness of COF shell on the plasmonic beads. d) PXRD pattern of SiO_2@Au@$COF_{Hedgehog}$ composites.

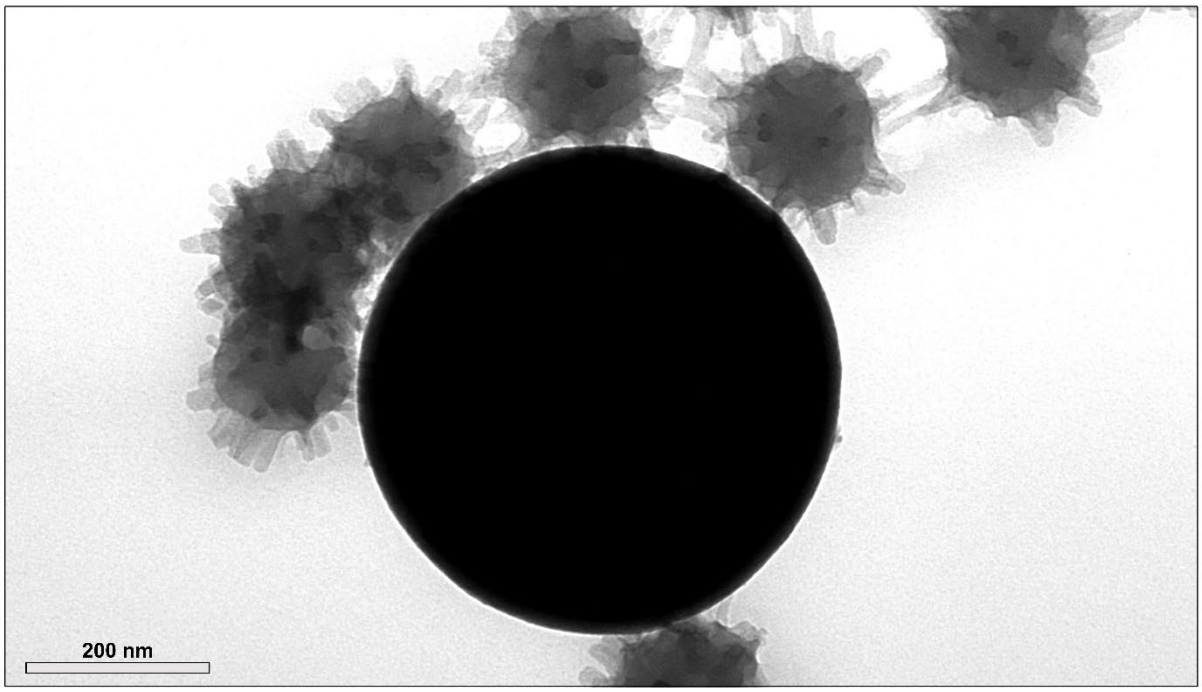

Figure S16. TEM images of $COF_{Hedgehog}$ particle islands on the surface of SiO_2 bead.

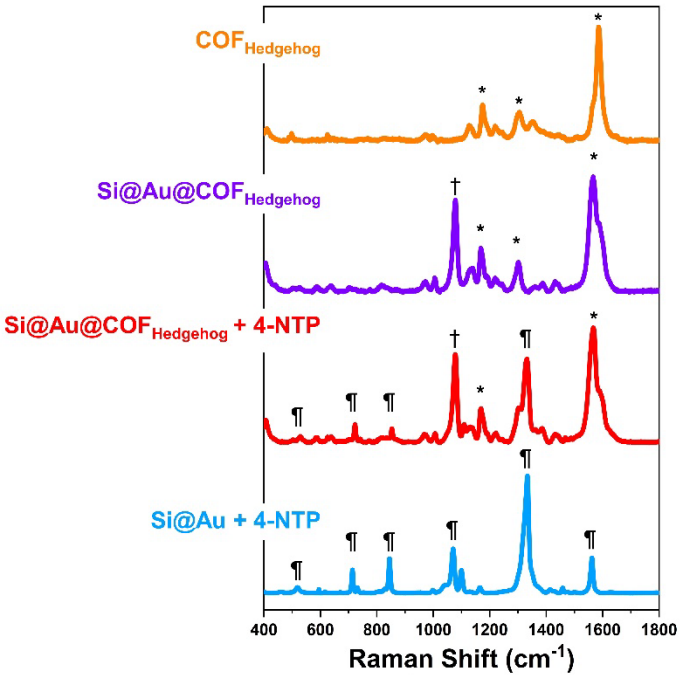

Figure S17. Raman spectra of $COF_{Hedgehog}$ particles and SERS spectra of SiO_2@Au@$COF_{Hedgehog}$ composites alone, SiO_2@Au@$COF_{Hedgehog}$ + 4-NTP, and SiO_2@Au + 4-NTP. Marks indicate the dominant bands for the samples: (*) = COF, (†) = 4-ATP, and (¶) = 4-NTP.

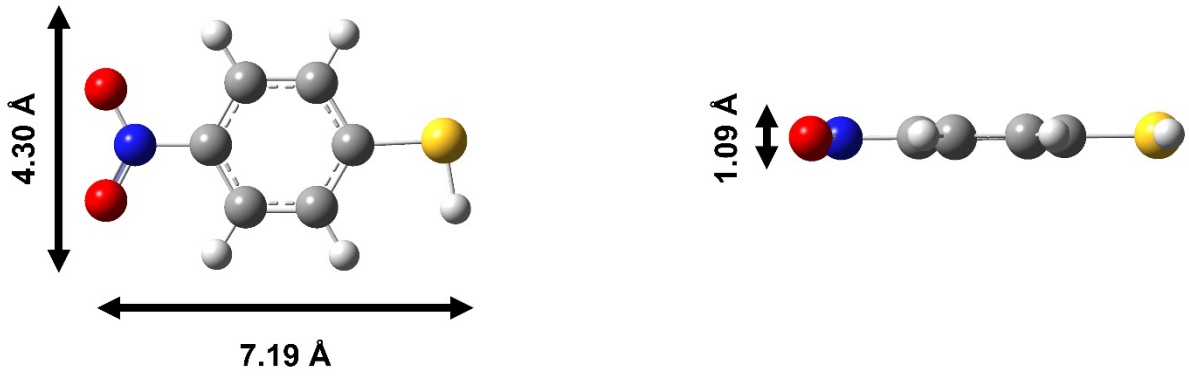

Figure S18. DFT calculations of the size of 4-NTP probe at the B3LYP 6-311G(d,p) level of theory. Color code: blue = N, red = O, and yellow = S.

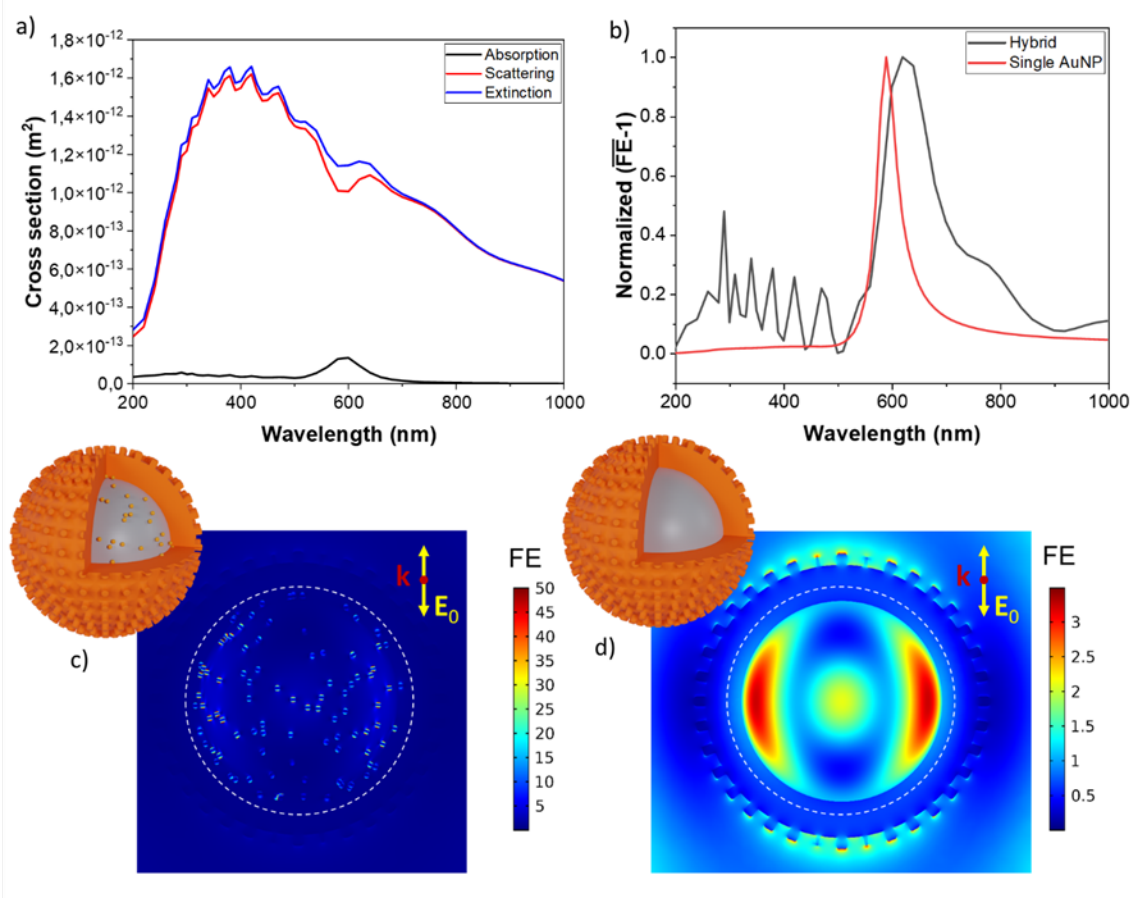

Figure S19. **a)** Simulated spectra of interaction cross sections of SiO_2@Au@$COF_{Hedgehog}$ in water spectra. **b)** Normalized volume-averaged field enhancement spectra for the hybrid (black line) and a single Au NP (red line) immersed in a medium with the same n_{COF}. **c,d)** Field enhancement maps at 785 nm for the SiO_2@Au@$COF_{Hedgehog}$ hybrid and a SiO_2@COF system, respectively. The insets present are 3D renders of the geometry used for the calculations. The size of the different elements of the hybrids are described below. Please note that the colour scale in panel *c* is capped well below the maximum value (see hot spots in Fig. 6c) for clarity of presentation.

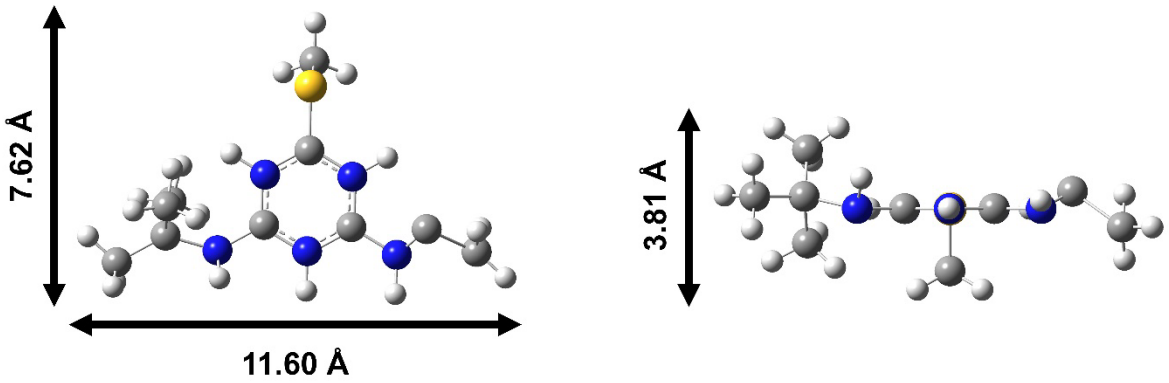

Figure S20. DFT calculations of the size of terbutryn at the B3LYP 6-311G(d, p) level of theory. Colour code: Blue = N, and Yellow = S.

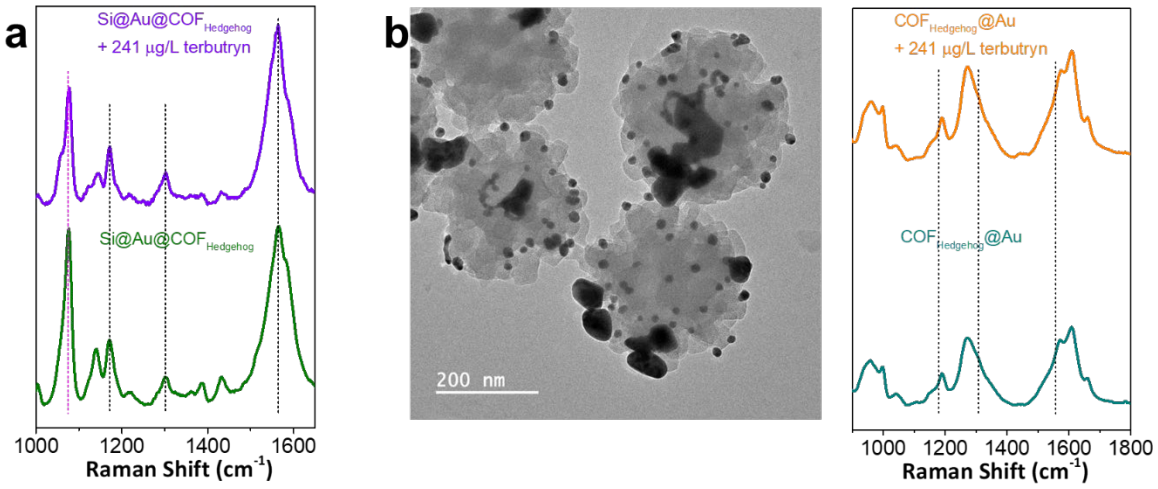

Figure S21. a) Direct SERS detection of 241 µg/L terbutryn using SiO_2@Au@$COF_{Hedgehog}$ composite (purple spectrum). For comparison, the SERS spectrum of SiO_2@Au@$COF_{Hedgehog}$ composite was included in the graph (green spectrum). No relevant differences were observed between the two spectra. Black and pink dashed lines indicated the most relevant COF peaks and 4-ATP, used as a linker, respectively. **b)** TEM of COF@Au composite and SERS spectra of COF@Au in the absence and presence of 241 µg/L terbutryn. Black dashed lines indicate the position of characteristic peaks of $COF_{Hedgehog}$ particles before gold growth.

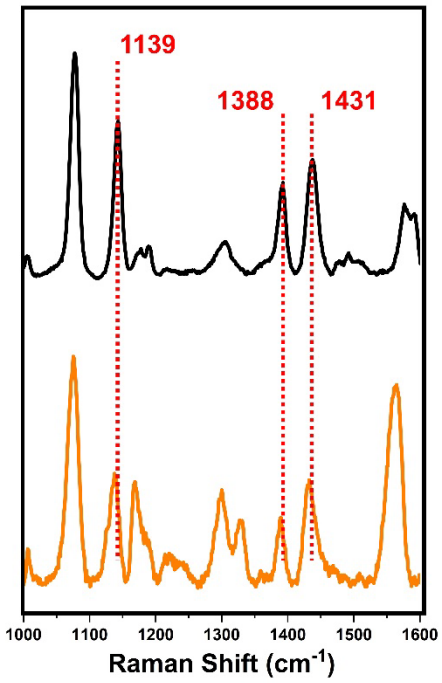

Figure S22. SERS spectra of 4,4-dimercaptoazobenzene (DMAB) (top), and 4-NTP-functionalized SiO_2@Au@$COF_{Hedgehog}$ composites after incubation with 241 μg/L terbutryn (bottom). The SERS spectra were acquired upon excitation with a 785 nm laser line. The red dashed lines indicate the characteristics peaks of DMAB.

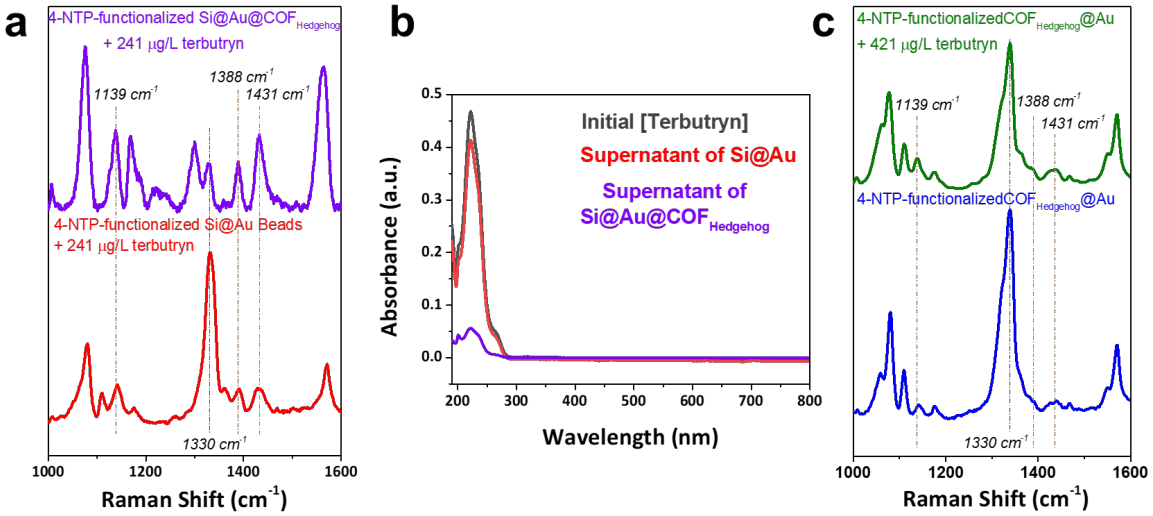

Figure S23. a) Comparison SERS spectra of 4-NTP-functionalized SiO_2@Au@$COF_{Hedgehog}$ (violet) and SiO_2@Au (red) after terbutryn addition of equal concentration (10^{-6} M = 241 μg/L). Grey and orange dashed lines indicate the characteristic peaks of 4-NTP and DMAB, respectively. Clearly, the characteristic peaks of DMAB are only evident when terbutryn is incubated with SiO_2@Au@$COF_{Hedgehog}$. SERS spectra were acquired upon excitation with 785 nm laser line. **b)** Comparison of UV–Vis spectra of the supernatant of 4-NTP-functionalized SiO_2@Au@$COF_{Hedgehog}$ (violet) and SiO_2@Au (red) after equal concentration of terbutryn addition. For a better comparison, UV–Vis spectra of 241 μg/L terbutryn (black) is also given. **c)** SERS spectra acquired upon excitation with 785 laser line of 4-NTP using a different configuration of SERS substrate, AuNPs-coated $COF_{Hedgehog}$ ($COF_{Hedgehog}$@Au). Slightly different spectra were observed in 4-NTP in the absence (blue spectrum) and presence (green spectrum) of 241 μg/L terbutryn: a slight decrease in the peak intensity centred at 1330 cm^{-1} (nitro group stretching). Green and orange dashed lines indicate the characteristic peaks of 4-NTP and DMAB, respectively.

Table S3. Revision of composites involving COF and plasmonic nanostructures for SERS applications.

COF Type (shape)	*Plamonic nanostructure*	*Composite configuration*	*Application (LoD)*	*Reference*
TAPB-DMTP COF (spherical sub-micro particles)	AgNPs	AgNPs-coated COF	SERS-Based aptasensor for patulin detection (54.4 ng/L)	[6]
TpPa-1 COF (bulk)	AuNPs	AuNPs-coated COF	Nanozyme for the reduction of 4-nitrophenol for the detection of Acetylcholine (0.3 pM – 43.9 ng/L)	[7]
TpDb-AO COF (bulk flakes)	AgNPs	AgNPs-coated COF	Uranium direct detection (3.72 µg/L)	[8]
TpPa COF (spiked microparticles)	AgNPs	AgNPs-coated COF	DNA bases (adenine) direct detection (0.026 pM – 40.5 ng/L)	[9]
TAPB-PDA COF (spherical microparticles)	AgNPs	AgNPs-coated COF	Amoxicillin direct detection (279 ng/L)	[10]
TAPB-DVA COF (urchin-like shape)	Au@Ag NPs core@shell	Au@AgNPs-coated COF	Sulfamethoxazole (2.03 µg/L) and polystyrene nanoplastics (29 µg/L) direct detection	[11]
TAPB-DMTA COF (flower-like sub-micron particles)	AgNPs	AgNPs-coated COF	Malachite green (38 µg/L) and crystal violet (18 µg/L) direct detection	[12]
3D chiral SU-1 COF	AuNPs	AuNPs-coated COF	SERS-Based enantioselective discrimination (n.d.)	[13]
TPB-DVA COF (cubic particles)	AgNPs	AgNPs-coated COF	Benzoic acid direct detection (3.72 µg/L)	[14]
Ultrathin 2D-phorphyrin-COFs	-	Plasmonic properties from the COF	Designing a new plasmonic material, which has an Enhancement Factor of 5	[15]

PPD-TFB COF (bulk)	Au nanoflowers	COF layer-coated Au nanoflowers	Single-molecule detection by controlling the nanogap between Au nanoflowers via COF thickness	[16]
TAPB-DMTP COF (hedgehog-shaped)	*AuNPs-coated SiO_2 bead*	*COF shell-coated AuNPs/SiO_2 (SiO_2@Au@ $COF_{Hedgehog}$)*	*Indirect detection of terbutryn (241 ng/L)*	*This study*

Table S4. Comparison of the SERS detection approaches reported in the literature with the current study for triazine detection.

Triazines	*Matrix*	*Technique*	*Substrate*	*Laser*	*LODs*	*Study*
Terbutryn	*Ultrapure water*	*Indirect SERS by reducing Nitro group to amine group*	*SiO_2@Au@$COF_{Hedgehog}$*	*785 nm (7.7 mW)*	*241 ng/L (1 nM)*	*Current Study*
Atrazine Prometryn Simetryn	Ultrapure water	Direct SERS	Ag NPs	514.5 nm (40 mW)	1 mg/L	[17]
Prometryn Simetryn	Rice Wheat	Direct SERS	Molecularly imprinted polymer with integrated AuNPs	785 nm	20 µg/L	[18]
Prometryn	Ultrapure water	Direct SERS	Ag NPs	532 nm	28 µg/L (0.12 µM) at pH 11 128 µg/L (0.53 µM) at pH 7	[19]
Simetryn	Lake water	Direct SERS	Single-well carbon nanotubes (SWCNTs) decorated with AuNPs	785 nm (60 mW)	2 µg/L	[20]

3. Theoretical methodology

Finite element method (FEM) simulations for the $COF_{Hedgehog}$ and SiO_2@Au@$COF_{Hedgehog}$ systems were used to solve their classical electrodynamic response, using the COMSOL Multiphysics software. From these results, we calculated their theoretical extinction spectra and the near-field enhancement around the Au NPs. For the latter, we computed the average field enhancement for a specific volume immediately surrounding the AuNPs, the relevant region in which the SERS signal will originate. Explicitly, the FE and the $\overline{\mathrm{FE}}$ were computed as follows, where **E(r)**, E_0, and V are, respectively, the electric field measured at point **r**, the amplitude of the incoming planewave, and the volume of a thin shell extending from SiO_2 surface to the surface of a sphere 15 nm over the AuNPs (Figure 6b).

$$FE = \frac{\left|\mathbf{E}(\mathbf{r})\right|^2}{E_0^2}; \quad \overline{FE} = \frac{1}{V}\int_V \frac{\left|\mathbf{E}(\mathbf{r})\right|^2}{E_0^2} dV$$

The permittivity for gold was taken from experimental values in the literature,[21] while the refractive index of the dielectrics was taken as n_{SiO2} = 1.45, as n_{H2O} = 1.33, and n_{COF} = 2. Consequently, only the gold was modelled as an absorbing material, and the optical absorption of SiO_2 and the COF was not included in the model. In absence of sufficient optical characterization of the COF material in the literature, we chose its refractive index to match the experimentally observed redshift of the AuNPs in our experiment.

The $COF_{Hedgehog}$ model has a 325 nm core diameter and cylindrical spikes with 100 nm in length and 28 nm in width. The SiO_2@Au@$COF_{Hedgehog}$ model has a SiO_2 sphere of 488 nm in diameter, gold nanoparticles of 14.5 nm in diameter and a COF shell with a thickness of 88 nm and cylindrical spikes with 27 nm in length and 25 nm in width.

Author contributions

Tolga Zorlu – Investigation, Formal analysis, Visualization, Writing – original draft

Maedeh Anisi – Investigation, Formal analysis

Monica Quarato – Investigation, Formal analysis

Ana Vieira - Investigation

Jesús Giráldez-Martínez – Investigation, Formal analysis

Carlos Gonçalves – Investigation, Formal analysis

Aitor Alvarez – Investigation

Tania Prieto – Investigation, Visualization, Writing – review & editing

Dana D. Medina – Investigation, Formal analysis

Lucas V. Besteiro – Investigation, Formal analysis, Supervision, Methodology

Miguel A. Correa-Duarte – Resources, Supervision, Writing – review & editing

Begoña Espiña – Resources, Supervision, Writing – review & editing

Laura Rodriguez-Lorenzo – Conceptualization, Project administration, Supervision, Resources, Writing – review & editing

Laura M. Salonen – Conceptualization, Project administration, Supervision, Resources, Writing – review & editing

References

1. M. e. Frisch, G. Trucks, H. B. Schlegel, G. Scuseria, M. Robb, J. Cheeseman, G. Scalmani, V. Barone, G. Petersson and H. Nakatsuji, *Journal*, 2016.
2. B. Enustun and J. Turkevich, *Journal of the American chemical society*, 1963, **85**, 3317-3328.
3. J. Turkevich, P. C. Stevenson and J. Hillier, *Discussions of the Faraday Society*, 1951, **11**, 55-75.
4. L. M. Rossi, L. Shi, F. H. Quina and Z. Rosenzweig, *Langmuir*, 2005, **21**, 4277-4280.
5. P. P. Ghimire and M. Jaroniec, *Journal of Colloid and Interface Science*, 2021, **584**, 838-865.
6. Z. Guo, J. Ma, L. Yin, S. Xue, R. Zhou, C. Sun, C. Wang, H. Jayan, N. Yosri and X. Zou, *Journal of Food Composition and Analysis*, 2025, **148**, 108329.
7. C. Fu, Y. Li, X. Lei, J. Su, Y. Chen, Y. Wu, W. Shi, X. Tan, Y. Li and Y. M. Jung, *Analytical Chemistry*, 2024, **96**, 18585-18589.
8. X. Guo, X. Wang, S. Wen, H. Wu, J. Wang, M. Wang, D. He, F. Zhao, J. Liu, X. Yang and S. Wang, *Advanced Functional Materials*, 2025, **35**, 2500901.
9. C. Fu, S. Jiang, S. Zhuo, J. Qiu, H. Luo, Y. Wu, Y. Li and Y. M. Jung, *Analytical and Bioanalytical Chemistry*, 2024, **416**, 5295-5302.
10. K. Chen, C. Ma, G. Chen, T. Yang, H. Gao, L. Li, Z. Yang, J. Cao, C. Zheng and L. Ma, *Spectrochimica Acta Part A: Molecular and Biomolecular Spectroscopy*, 2024, **313**, 124165.
11. X. Yuan, W. Wang, M. Chen, L. Huang, Q. Shuai and L. Ouyang, *Chemical Communications*, 2024, **60**, 8840-8843.
12. Q. Wei, L. Shao, H. Pu and D.-W. Sun, *Journal of Food Measurement and Characterization*, 2024, **18**, 2903-2915.
13. J. Yang, S. Wei, T. Zhang, L. Wu, L. Jia, J. Dong, C. Yuan, Y. Cui and X. Hou, *Journal of the American Chemical Society*, 2025, **147**, 28085-28097.
14. Z. Yang, C. Ma, J. Gu, Y. Wu, C. Zhu, L. Li, H. Gao, W. Yin, Z. Wang, Y. Zhang, Y. Shang, C. Wang and G. Chen, *Spectrochimica Acta Part A: Molecular and Biomolecular Spectroscopy*, 2022, **267**, 120534.
15. Y. Ying, M. Fang, C. Wang, Z. Yan, H. Xie, W. Wu, Z. Tang and Y. Liu, *Small*, 2025, **21**, 2501846.
16. M. Lv, X. Wu, W. Wang, D. Han, S. Chen, Y. Hu, Q. Zhang, Q. Wang and R. Wei, *ACS Sensors*, 2025, **10**, 1778-1787.
17. S. Bonora, E. Benassi, A. Maris, V. Tugnoli, S. Ottani and M. Di Foggia, *Journal of Molecular Structure*, 2013, **1040**, 139-148.
18. M. Yan, Y. She, X. Cao, J. Ma, G. Chen, S. Hong, Y. Shao, A. M. Abd El-Aty, M. Wang and J. Wang, *Microchimica Acta*, 2019, **186**, 143.
19. R. J. G. Rubira, L. N. Furini, C. J. L. Constantino and S. Sanchez-Cortes, *Vibrational Spectroscopy*, 2021, **114**, 103245.
20. Z. Deng, H. Liu, Y. Wang and X. Chen, *Analytical Methods*, 2015, **7**, 2190-2195.
21. P. B. Johnson and R.-W. Christy, *Physical review B*, 1972, **6**, 4370.